Study of the properties of *Ru*-isotopes using the proton-neutron interacting boson model (IBM-2)

Altaf Abdul Majeed Al-Rahmani*

Date of acceptance 28 / 2 / 2010

Abstract:
The proton-neutron interacting boson model (IBM-2) has been used to make a schematic study of the Ruthenium (Ru) isotopes of mass region around $A=100$ with $Z=44$, and $54\le N\le 64$. For each isotope of Ru the values of the IBM-2 Hamiltonian parameters, which yield an acceptable results for excitation energies in comparison with those of experimental data, have been determined. Fixed values of the effective charges ($e_\pi = e_\nu = 0.102\ e.b.$) and of the proton and neutron g factors ($g_\pi = 1.0\ \mu_N$ and $g_\nu = 0.42\ \mu_N$) have been chosen for all isotopes under study. The calculated electric transitions, the magnetic dipole moments $\mu_{2_1^+}$, $B(E2)$ quadrupole moments of 2_1^+ state, $B(M1)$ transitions and $\delta(E2/M1)$ mixing ratios are in reasonable agreement with the experimental data.

Key word: Nuclear Structure Interacting Boson Model, Investigation of the Ru-isotpes Energies, B(E2) transition rates, and other properties. Model parameters as aSmooth function of neutron number

1. Introduction

One of the main objectives of the study of nuclear physics is to understand the structure of nuclei. One of the interesting features of the IBM-2 is the prediction of a large class of states which are non-symmetric under the interchange of neutron bosons and proton bosons, and which are outside the model of the IBM-1. The lowest six excited 2^+ levels of the $^{122-130}Te$ nuclei have been investigated experimently [1]. These levels have been identified and their decay properties have been characterized from gamma-ray excitation functions. In addition, the lifetime of these levels have been deduced using the doppler-shift attenuation method. Electromagnetic transition rates and E2/M1 multipole mixing ratios from the $2_{2-6}\rightarrow 2_1$ transitions have been examind to identify the lowest mixed-symmetry states in these nuclei. The summed M1 stregth from the $2_{2-6}\rightarrow 2_1$ level agree rather well with neutron-proton interacting boson model predictions in the U(5) or O(6) limits for these Te nuclei. The energy spectra of the ($^{121-127}Xe, ^{121-127}I$) are cosidered in the (IBFM-2). Electromagnetic transition probabilities and branching ratio in odd $^{121-127}I$ isotopes have been investigated in [2]. Genilloud et al.[3] measured lifetime of excited states in ^{100}Ru. The absolute transition rates were extracted for these states.

Parallel with these theoretical developments, several experiments were carried out to test the propreties of the low lying collective states in some nuclei of the IBM-2 [4-9]. The experimental work of Ref [10] was

*Physics Department, College of Science for Women, University of Baghdad.

made to measure the absolute $M1$ and $E2$ transition strength in ^{94}Mo nucleus. The determination of branching ratios and $E2/M1$ mixing ratios in this nucleus was also made. Besides an identification of some mixed symmetry states was a chieved. These expereimental result were in reasonable agreement with the calculations of IBM-2.

The emphasis in this work is on describing overall trends with constant parameters, rather than obtaining the best possible fit to the experimental data for each nucleus. This is done in an effort to find a set of IBM-2 Hamiltonian parameters which is appropriate for the entire isotopic chain.In the presesnt work, the calculations have been performed for the transitional nuclei $[U(5) \rightarrow O(6)]$ of $Ru-$isotopes (with $Z = 44$ and $54 \le N \le 64$) and devoted to study (i) the energy spectra and consequently the excitation energy of the lowest symmetric and mixed symmetric states (ii) the electric properties such as the quadrupole moment of the first excited state 2_1^+ and the $E2$ transition rates (iii) the magnetic properties which include the magnetic dipole moment of the first excited state 2_1^+, the $M1$ transition strengths and the mixing ratios.

2. The interacting proton-neutron model

The proton- neutron interacting boson model, which is known as IBM-2, can make an explicit distinction between proton-and neutron -bosons. The Hamiltonian operator in the IBM-2 has the form

$$\hat{H} = \hat{H}_\pi + \hat{H}_\nu + \hat{V}_{\pi\nu} \quad (1)$$

where the first and second terms are describing the proton and neutron bosons while the third term is for describing the proton-neutron interaction. A simple schematic hamiltonian guided by microscopic consideration is given by [11]

$$\hat{H} = \epsilon_\pi \left(\hat{d}^+ \times \hat{\tilde{d}}\right)_\pi + \epsilon_\nu \left(\hat{d}^+ \times \hat{\tilde{d}}\right)_\nu + \hat{V}_{\pi\pi} + \hat{V}_{\nu\nu} + K\hat{Q}_\pi.\hat{Q}_\nu + M_{\pi o}, \quad (2)$$

where ϵ_π and ϵ_ν are the excitation energies for proton and neutron $d-$bosons respectively, $\left(\hat{d}^+ \times \hat{\tilde{d}}\right)_\pi$ and $\left(d^+ \times \tilde{d}\right)_\nu$ are the $d-$boson number operators for protons and neutrons respectively, K is the strength of the quadrupole-quadrupole interaction between proton and neutron bosons, Q_π and Q_ν are the quadrupole operators for proton and neutron bosons, respectively. Here Q_ρ ($\rho = \pi$ or ν) is given by

$$\hat{Q}_\rho = \left(\hat{d}^+ \times \hat{\tilde{s}} + \hat{s}^+ \times \hat{\tilde{d}}\right)_\rho^{(2)} + \chi_\rho \left(\hat{d}^+ \times \hat{\tilde{d}}\right)_\rho^2, \quad (3)$$

where $s^+, \tilde{s}, d^+$ and $\tilde{d}$ are operators which create and annihilate s and d bosons respectively and χ_ρ is the structure parameter. The residual two-body interaction between the like bosons is

$$V_{\rho\rho} = \sum_{L=0,2,4} \frac{1}{2}(2L+1)^{\frac{1}{2}} C_L^\rho \times \left[\left(\hat{d}_\rho^+ \times \hat{d}_\rho^+\right)^{(L)} . \left(\hat{\tilde{d}}_\rho \times \hat{\tilde{d}}_\rho\right)^{(L)}\right]^{(0)} \quad (4)$$

The C_L^ρ parameter is well known to effect only minor details of the energy spectrum. Finally $M_{\pi\nu}$ is the so-called Majorana operator and given by [13]

$$M_{\pi\nu} = \xi_2 \left[\hat{s}_\nu^+ \times \hat{d}_\pi^+ - \hat{s}_\pi^+ \times \hat{d}_\nu^+\right]^{(2)} . \left[\hat{\tilde{s}}_\nu \times \hat{\tilde{d}}_\pi - \hat{\tilde{s}}_\pi \times \hat{\tilde{d}}_\nu\right]^{(2)}$$

$$-2\sum_{k=1,3}\xi_k\left[\hat{d}_\nu^+\times\hat{d}_\pi^+\right]^{(k)}.\left[\tilde{\hat{d}}_\nu\times\tilde{\hat{d}}_\pi\right]^{(k)} \quad (5)$$

where ξ_k $(k=1,2,3)$ are Majorana parameters since the Majorana interaction has been introduced to push the states with a mixed $\pi\nu$ symmetry character to higher energies thereby at the same time reducing the possible $F-$spin admixing in low-lying states [12]. The energy levels are obtained by diagonalizing the Hamiltonian of eq. (2) and then allowing the parameters $\in_\pi$, $\in_\nu$, K, χ_π, χ_ν and C_L to vary until a best fit to the experimental spectrum is obtained.

3. Energy spectra

The values of the parameters of the transitional nuclei $SU(5)\rightarrow O(6)$ of the $Ru-$isotopes employed in the hamaltonian of IBM-2 are displayed in Table (1).

Table (1): The hamiltonian parameters of IBM-2 for $Ru-$isotopes.

Parameters	^{98}Ru	^{100}Ru	^{102}Ru	^{104}Ru	^{106}Ru	^{108}Ru
N_ν	**2**	**3**	**4**	**5**	**6**	**7**
N_π	**3**	**3**	**3**	**3**	**3**	**3**
$\in$	**0.935**	**0.910**	**0.865**	**0.760**	**0.690**	**0.660**
k	**-0.163**	**-0.155**	**-0.145**	**-0.140**	**-0.140**	**-0.140**
χ_ν	**-0.800**	**-1.000**	**-0.900**	**-0.900**	**-1.000**	**-0.800**
χ_π	**0.400**	**0.400**	**0.400**	**0.400**	**0.400**	**0.400**
$C_{0\nu}$	**-0.950**	**-0.853**	**-0.760**	**-0.316**	**-0.110**	**-0.060**
$C_{2\nu}$	**0.185**	**0.135**	**-0.100**	**-0.126**	**-0.070**	**-0.050**
$C_{4\nu}$	**-0.740**	**-0.238**	**-0.127**	**-0.075**	**-0.055**	**-0.050**
ξ_1	**0.100**	**0.100**	**0.100**	**0.100**	**0.100**	**0.100**
ξ_2	**0.100**	**0.100**	**0.100**	**0.100**	**0.100**	**0.100**
ξ_3	**0.100**	**0.100**	**0.100**	**0.100**	**0.100**	**0.100**

The calculated energy spectra of $Ru-$isotopes are plotted in Fig. (1) as a function of the neutron numbers. A detailed comparison of the ground, gamma and beta bands with experiment are shown in Figs (1a), (1b) and (1c), respectively. Figure (1a) shows a good agreement between the calculated energies of 2^+, 4^+, 6^+ and 8^+ states and those of the experimental data while the state 10^+ deviates significantly from the data at $^{98}Ru_{54}$ isotope. However, we should be careful in comparing theory with experiment, since all calculated states have a collective nature, whereas some of the experimental states may have a particle-like structure. For example in $^{98}Ru_{54}$ isotope, the particle-like structure of 10^+ state is confirmed by

the presence of a maximum in the energies at $^{100}Ru_{54}$. Fig. (1b) shows that the calculated energy of 3_1^+ and 5_1^+ states are predicted too high by IBM-2. This is a consequence of the presence of a Majorana term $M_{\pi\nu}$ in the Hamiltonian of IBM-2. The parameters of the Majorana force have chosen in such a way that it push up states that are not completely symmetric with respect to proton and neutron bosons. Fig. (c) shows that the experimental 0_2^+ states are very well described by the calculated result whereas, in general, the calculated 2_3^+ and 4_3^+ are in reasonable agreement with the experimental data in $Ru-$isotopes.

4. Electromagnetic properties

The electric quadrupole transition operater $\hat{T}(E2)$ of IBM-2 is given by [11]

$$\hat{T}(E2) = e_\pi \hat{Q}_\pi^\chi + e_\nu \hat{Q}_\nu^\chi \quad (6)$$

$$\hat{Q}_\rho^\chi = \left[\hat{d}^+ \times \hat{\tilde{s}} + \hat{s}^+ \times \hat{\tilde{d}}\right]_\rho^{(2)} + \chi_\rho \left[\hat{d}^+ \times \hat{\tilde{d}}\right]_\rho^{(2)} \quad (7)$$

It has been used for calculating the $E2$ transition rates and the quadrupole moments of the first excited 2^+ states $Q_{2_1^+}$ in $Ru-$isotopes. In the principle, the values of proton-boson e_π and neutron-boson e_ν effective charges could be different from each other and different for each nucleus. In the present work, fixed values of $e_\pi = e_\nu = 0.102\, eb$ in IBM-2 has been used for a chain of $Ru-$isotopes.

The calculated $B(E2; I_i \to I_f)$ transitions (the solid curves), in e^2b^2, is plotted in Fig. (2) as a function of neutron numbers of $Ru-$isotopes and compared with those of experimental data (the filled circles). The calculated $B(E2,2_1^+ \to 0_1^+)$, $B(E2,4_1^+ \to 2_1^+)$ transitions of figures (2a), (2b), respectively, agree quite well with those of the experimental data and they show an increase in their values with the increasing of the neutron numbers since this behavior is in consistent with the experiment. In figure (2c), the $B(E2,2_2^+ \to 2_1^+)$ transition demonstrates an agreement with that of the experimental data for $N = 54$ and 60, but overestimates the data for $N = 56$ and 62. It is obvious from figure (2d), that the calculated $B(E2,2_2^+ \to 0_1^+)$ transition underestimates the data. This discrepancy may be attributed to considering a fixed value of effective charge ($e_\pi = e_\nu = 0.102 \quad eb$) in the boson $E2$ operator of eq. (6) for all $Ru-$isotopes.

For the sake of completeness, the other $B(E2)$ properties such as the ratios

$$\frac{B(E2;3_1^+ \to 4_1^+)}{B(E2;3_1^+ \to 2_2^+)}, \quad \frac{B(E2;2_2^+ \to 2_1^+)}{B(E2;2_1^+ \to 0_1^+)} \text{ and } \frac{B(E2;4_1^+ \to 2_1^+)}{B(E2;2_1^+ \to 0_1^+)}, \frac{B(E2;2_2^+ \to 0_1^+)}{B(E2;2_2^+ \to 2_1^+)},$$

which are displayed in Fig. (3), are calculated and compared with those of experimental data. The open squares are the calculated ratios in the frame work of IBM-2 while the filled circles are those of the experimental data [22, 23].

The quadrupole moments of the first excited 2_1^+ state $Q_{2_1^+}$ for

$Ru-$isotopes are also studied in this work and presented in Fig. (4). In this figure the calculated $Q_{2_1^+}$ is represented by the solid curve. While the filled circles are those of the experimental, It is very clear that the general feature of these experimental data is an increase in the negative quadrupole moment with increasing the neutron number. Inspection of this figure provides an indication that the experimental data of the quadrupole moments of the first excited 2_1^+ state are very well described by the calculation of IBM-2 throughout all the considered $Ru-$isotopes. It is seen that the calculated $Q_{2_1^+}$ of IBM-2 gives a remarkable agreement, in both behavior and magnitude, in comparison with those of experimental data.

The properties of the magnetic dipole operator such as the $B(M1)$ transition and the magnetic dipole moment of the first excited 2_1^+ ($\mu_{2_1^+}$) state as well as the $\delta-$mixing ratios are also studied by the present work of IBM-2. Here, the boson $M1$ operator,

$$\hat{T}(M1)=\sqrt{\frac{3}{4\pi}}\left(g_\pi \hat{L}^\pi + g_\nu \hat{L}^\nu\right) \tag{8}$$

is used to reproduce these properties. However, these properties are exclusively determined by the parameters of g_π and g_ν factors. In this study a fixed values for g_π=0.25 μ_N and g_ν=0.085 μ_N is chosen as a first choice to reproduce these properties throughout all $Ru-$isotopes under study. Since these values have been determined from the comparison between the calculated $B(M1;2_2^+ \rightarrow 2_1^+)$ of IBM-2 and that of the experimental result in the $^{104}Ru-$ isotope [18].

The comparison between the calculated $B(M1)$ transitions and $\mu_{2_1^+}$ moments of IBM-2 model and those of the experimental data [14-18] is presented in Table (2). A clear picture could not be drawn for the properties of the $B(M1)$ transition in the $Ru-$isotopes due to the lack of experimental data. Table (2) shows that the calculated $\mu_{2_1^+}$ denoted by Th1, obtained using the first choice of g_π=0.25 μ_N and g_ν=0.085 μ_N, are not in agreement with those of experimental data for all considered $Ru-$isotopes. An improvement results for the calculated $\mu_{2_1^+}$ denoted by Th2 could be obtained due to adopting a second choice of g_π and g_ν such as g_π=1.00 μ_N and g_ν=0.42 μ_N. These values have been obtained from the comparison between the calculated magnetic dipole moments of the first excited state 2_1^+ and that of the experimental data in the $^{102}Ru-$ isotope [17]. As it is seen from Table (2) that the experimental data of $\mu_{2_1^+}$ are well explained by the calculated $\mu_{2_1^+}$ of IBM-2 using the second choice of g_π and g_ν.

The $\delta-$mixing ratios in the considered Ru-isotopes is also studied here and defined as

$$\delta(E2/M1)=0.832E_\gamma \times \Delta(E2/M1) \tag{9}$$

Where E_γ is in MeV and $\Delta(E2/M1)$ is in eb/μ_N and defined as the ratio of the reduced $E2$ matrix element to the $M1$ matrix element, i.e.

$$\Delta(E2/M1)=\frac{\left\langle f\left\|\hat{T}(E2)\right\|i\right\rangle}{\left\langle f\left\|\hat{T}(M1)\right\|i\right\rangle} \tag{10}$$

In Tables (3) to (8), the comparison between the experimental $\delta(E2/M1)$ mixing ratios [25,30-32] and those obtained by the present calculations of the IBM-2 using our first choice of g_π=0.25 μ_N and g_ν=0.085 μ_N are explored for all considered $Ru-$isotopes. In general, these Tables demonstrate that the absolute magnitudes of the calculated results for the $\delta(E2/M1)$ mixing ratios are in reasonable agreement with those of experimental data. However, predicting the sign of these $\delta(E2/M1)$ mixing ratios is a common problem in the IBM-2 model in spite of the reproduction of some of these $\delta(E2/M1)$ mixing ratios correctly.

Table (2): The $B(M1;I_i \to I_f)$ values, in the unit of (μ_N^2), and the magnetic dipole moments for the 2_1^+ states ($\mu_{2_1^+}$), in the unit of (μ_N), for $Ru-$isotopes obtained by IBM-2 model. The effective g-factors are taken as g_π=0.25 μ_N and g_ν=0.085 μ_N for the calculations of $B(M1)$ and $\mu_{2_1^+}$ (Th1) and as g_π=1.00 μ_N and g_ν=0.42 μ_N for the calculations of $\mu_{2_1^+}$ (Th2). The experimental values for $B(M1)$ and for $\mu_{2_1^+}$ are taken from Refs [14-18].

$I_i \to I_f$	^{98}Ru $B(M1)$	^{100}Ru $B(M1)$	^{102}Ru $B(M1)$	$B(M1)$ ^{104}Ru	$B(M1)$ ^{106}Ru	^{108}Ru
$1_1^+ \to 2_1^+$	0.0003	0.0007	0.0007	0.0009	0.0016	0.0006
$2_1^+ \to 2_2^+$	0.0036 Exp: 0.0033 ± 0.0006	0.0016 Exp: 0.0041 ± 0.007	0.0007 Exp: $\leq 10^{-4}$	0.0004 Exp: 0.0004± 0.00005	0.0003	0.0002
$2_1^+ \to 2_3^+$	0.0075	0.0007	0.0002	0.0005	0.0004	0.0004
$2_1^+ \to 2_4^+$	0.0001	0.0086	0.0089	0.0075	0.0060	0.0006
$3_1^+ \to 2_1^+$	0.0001	0.0001	0.0001	0.0001	0.0001	0.0001
$3_2^+ \to 2_1^+$	0.0007	0.0005	0.0003	0.0003	0.0005	0.0002
$3_1^+ \to 2_2^+$	0.0031	0.0027	0.0007	0.0003	0.0005	0.0002
$\mu_{2_1^+}$	Th1: 0.1695 Th2: 0.7170 Exp: 0.80 ± 0.08 0.78 ± 0.06	Th1: 0.1588 Th2: 0.6708 Exp: 1.02 ± 0.18	Th1: 0.1495 Th2 :0.6468 Exp: 0.69 ± 0.042	Th1: 0.1407 Th2: 0.6158 Exp: 0.82 ± 0.20 0.64 ± 0.02	Th1: 0.1313 Th2: 0.5828 Exp:	Th1: 0.1276 Th2: 0.5695 Exp: 0.54 ± 0.06

and $g_\nu = 0.085\ \mu_N$ in the IBM-2 for the $^{98}Ru-$ isotope. The experimentaldat are taken from Refs [30,14].

Table (3): A comparison between the experimental $\delta-$mixing ratios and those obtained by the present calculations using the parameters $e_\pi = e_\nu = 0.102\ e.b$, $g_\pi = 0.25\ \mu_N$

Transitions ($I_i \to I_f$)	mixing $\delta-$ ratios Experiment	mixing $\delta-$ ratios IBM-2
$2_2^+ \to 2_1^+$	$13.4^{+3.9}_{-2.5}$	0.903

$2_3^+ \to 2_1^+$	---------	-0.389
$2_4^+ \to 2_1^+$	---------	0.202
$3_1^+ \to 2_1^+$	---------	1.886
$3_2^+ \to 2_1^+$	---------	-0.002
$3_1^+ \to 2_2^+$	$0.4^{+1.7}_{-0.3}$	08.72
$1_1^+ \to 2_1^+$	-- ------	-0.330

Table (4): A comparison between the experimental $\delta-$mixing ratios and those obtained by the present calculations using the parameters $e_\pi = e_\nu = 0.102\ e.b$, $g_\pi = 0.25\ \mu_N$ and $g_\nu = 0.085\ \mu_N$ in the IBM-2 for the $^{100}Ru-$isotope. The experimentaldat are taken from Refs[15,16,31].

Transitions $(I_i \to I_f)$	mixing $\delta-$ ratios (Experiment)	$\delta-$ mixing ratios (IBM-2)
$2_2^+ \to 2_1^+$	3.5 ± 4, $2.4^{+0.47}_{-1.2}$	1.514
$2_3^+ \to 2_1^+$	$0.22^{+0.4}_{-0.6}$	-0.751
$2_4^+ \to 2_1^+$	--------	-0.0005
$3_1^+ \to 2_1^+$	$1.3^{+0.4}_{-0.9}$	1.335
$3_2^+ \to 2_1^+$	--------	-0.105
$3_1^+ \to 2_2^+$	--------	1.139
$1_1^+ \to 2_1^+$	--------	-0.043

Table (5): A comparison between the experimental $\delta-$mixing ratios and those obtained by the present calculations using the parameters $e_\pi = e_\nu = 0.102\ e.b$, $g_\pi = 0.25\ \mu_N$ and $g_\nu = 0.085\ \mu_N$ in the IBM-2 for the $^{102}Ru-$isotope. The experimentaldat are taken from Ref's [17,31].

Transitions $(I_i \to I_f)$	$\delta-$mixing ratios Experiment	$\delta-$mixing ratios IBM-2
$2_2^+ \to 2_1^+$	5^{+2}_{-3}	2.172
$2_3^+ \to 2_1^+$	$0.28^{+0.3}_{-0.3}$	-1.43
$2_4^+ \to 2_1^+$	--------	-0.029
$3_1^+ \to 2_1^+$	$-6.7^{+0.9}_{-0.7}$	2.225
$3_2^+ \to 2_1^+$	$-7.9^{+3.1}_{-1.4}$	0.246
$3_1^+ \to 2_2^+$	-7.2 ± 1	2.341
$1_1^+ \to 2_1^+$	--------	0.008

Table (6): A comparison between the experimental $\delta-$mixing ratios and those obtained by the present calculations using the parameters $e_\pi = e_\nu = 0.102\ e.b$, $g_\pi = 0.25\ \mu_N$ and $g_\nu = 0.085\ \mu_N$ in the IBM-2 for the $^{104}Ru-$isotope. The experimentaldat are taken from Ref's [18,31,25].

Transitions $(I_i \to I_f)$	$\delta-$mixing ratios Experiment	$\delta-$mixing ratios IBM-2
$2_2^+ \to 2_1^+$	$-8.5^{+2.5}_{-1.5}$	2.854
$2_3^+ \to 2_1^+$	0.45 ± 0.12	-0.573
$2_4^+ \to 2_1^+$	-0.03 ± 0.04	-0.070
$3_1^+ \to 2_1^+$	-3.2 ± 0.4	3.111
$3_2^+ \to 2_1^+$	0.12 ± 0.10	0.334
$3_1^+ \to 2_2^+$	--------	3.565
$1_1^+ \to 2_1^+$	--------	-0.043

Table (7): A comparison between the experimental $\delta-$mixing ratios and those obtained by the present calculations using the parameters $e_\pi = e_\nu = 0.102\ e.b$, $g_\pi = 0.25\ \mu_N$ and $g_\nu = 0.085\ \mu_N$ in the IBM-2 for the $^{106}Ru-$isotope. The experimentaldat are taken from Ref's [19,20,32] .

Transitions $(I_i \to I_f)$	$\delta-$mixing ratios Experiment	$\delta-$mixing ratios IBM-2
$2_2^+ \to 2_1^+$	$7.1^{+1.6}_{-11}$	3.245
$2_3^+ \to 2_1^+$	$0.24^{+0.13}_{-.0.12}$	0.104
$2_4^+ \to 2_1^+$	--------	0.076
$3_1^+ \to 2_1^+$	$-3.8^{+0.9}_{-1.6}$	3.428
$3_2^+ \to 2_1^+$	--------	0.546
$3_1^+ \to 2_2^+$	--------	3.061
$1_1^+ \to 2_1^+$	--------	-0.098

Table (8): A comparison between the experimental $\delta-$mixing ratios and those obtained by the present calculations using the parameters $e_\pi = e_\nu = 0.102\ e.b$, $g_\pi = 0.25\ \mu_N$ and $g_\nu = 0.085\ \mu_N$ in the IBM-2 for the $^{108}Ru-$isotope. The experimentaldat are taken from Ref's [21,32].

Transitions $(I_i \to I_f)$	$\delta-$mixing ratios Experiment	$\delta-$mixing ratios IBM-2
$2_2^+ \to 2_1^+$	$4.3^{+0.89}_{-0.63}$	3.977
$2_3^+ \to 2_1^+$	0.87 ± 0.66	-0.023
$2_4^+ \to 2_1^+$	$0.29^{+0.11}_{-0.14}$	0.206
$3_1^+ \to 2_1^+$	--------	7.537
$3_2^+ \to 2_1^+$	--------	0.784
$3_1^+ \to 2_2^+$	$-3.0^{+0.7}_{-1.4}$	3.700
$1_1^+ \to 2_1^+$	--------	-0.272

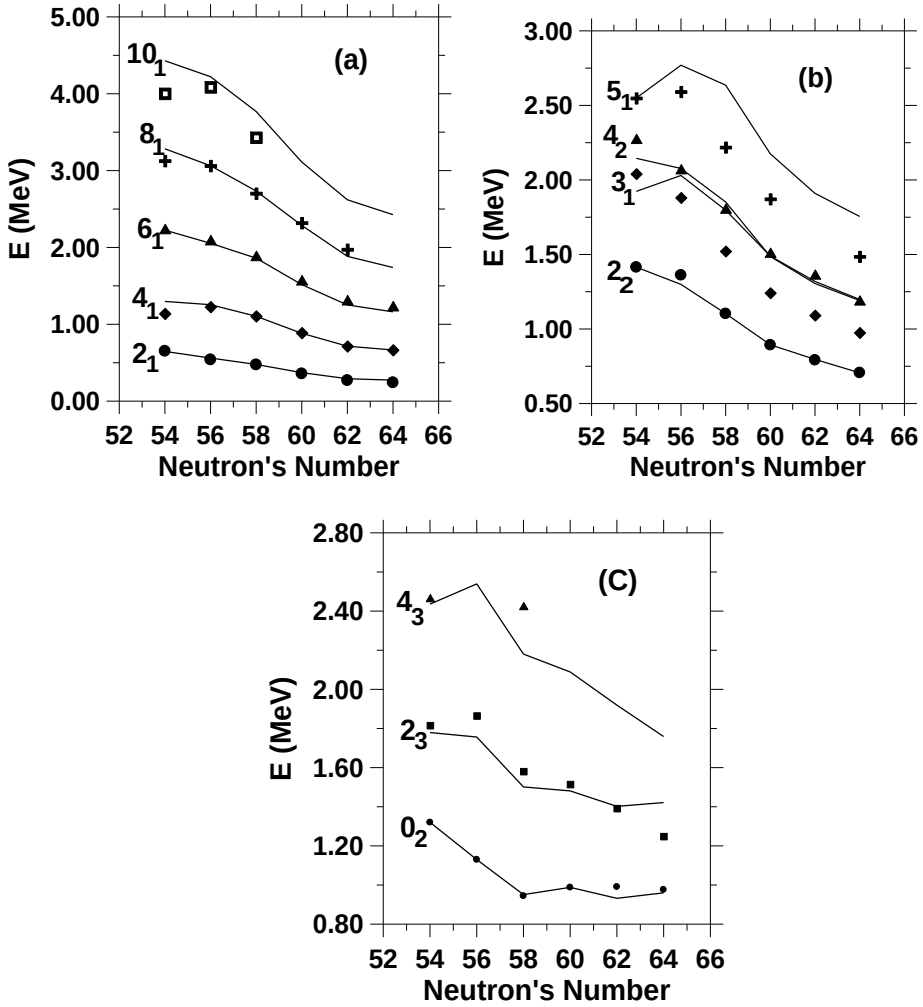

Fig. 1: The calculated energies of *Ru* -isotopes (solid lines) compared with those of experimental data (symbols) [14-21] for: (a) ground state band, (b) gamma state band and (c) beta state band.

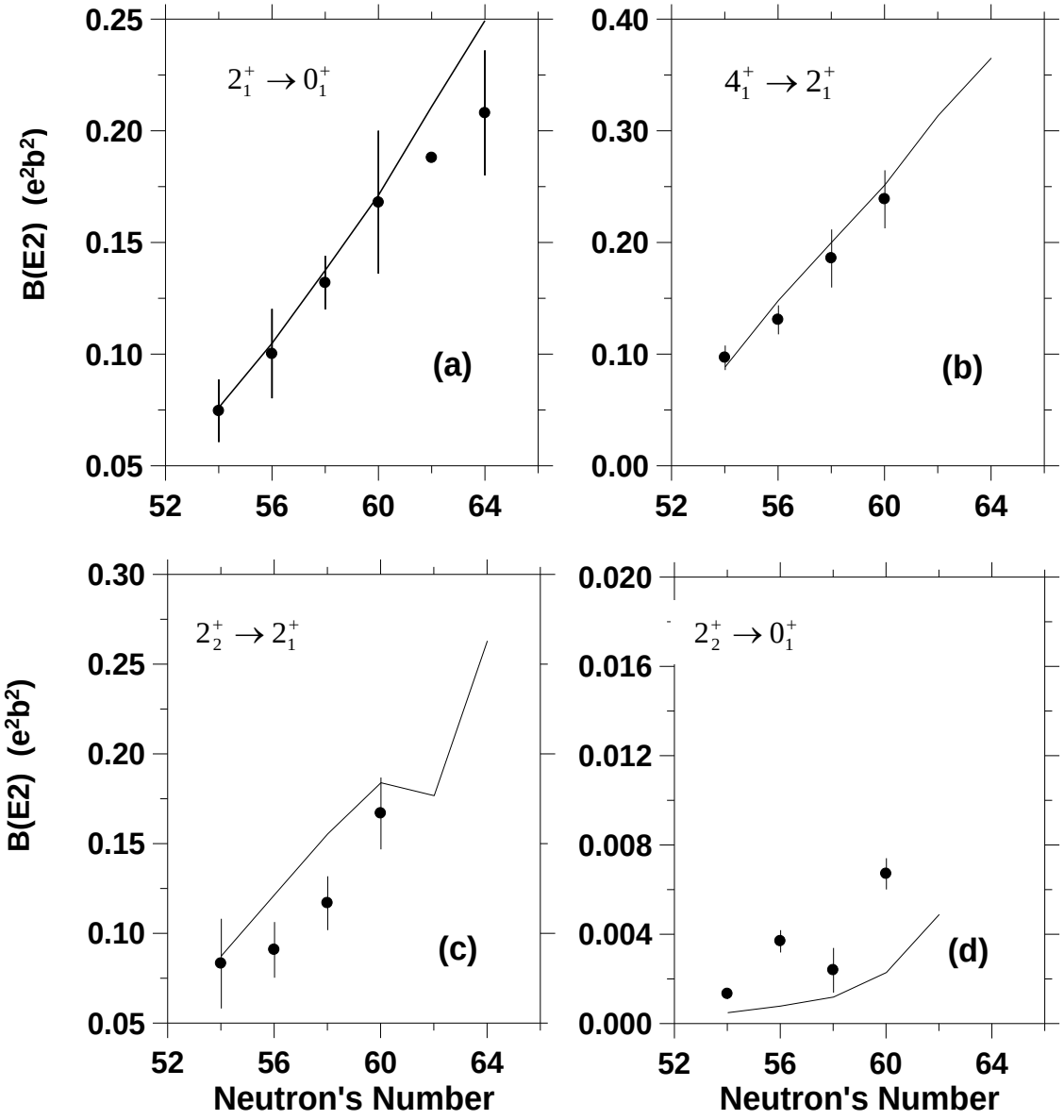

Fig. 2: The calculated B(E2) transitions (solid lines) compared with those of experimental data (symbols) [22, 23] in the *Ru* – isotopes.

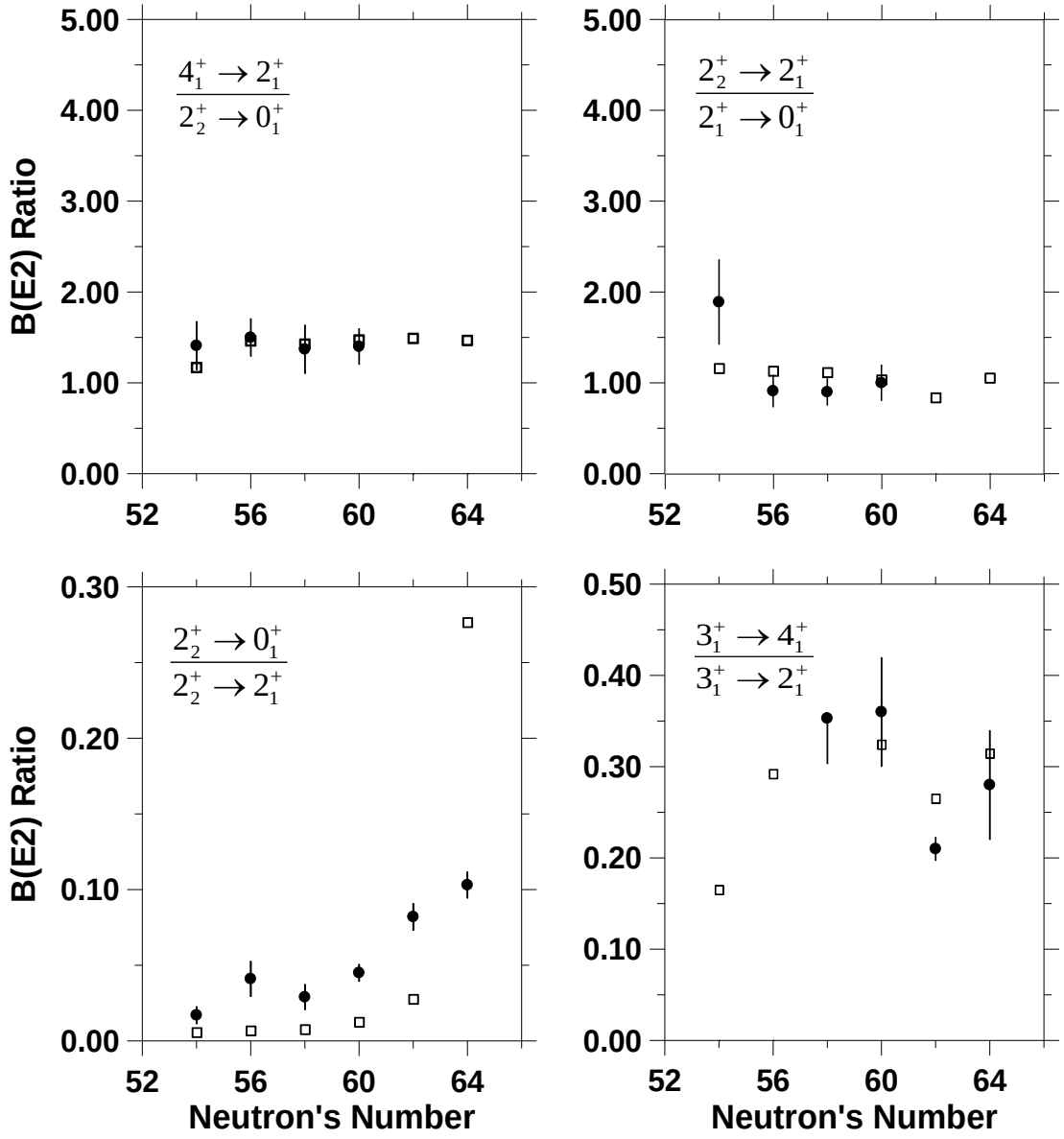

Fig. 3: The calculated B(E2) ratios (open squares) compared with those of experimental data (solid circles) [24-27] in the $Ru-$isotopes.

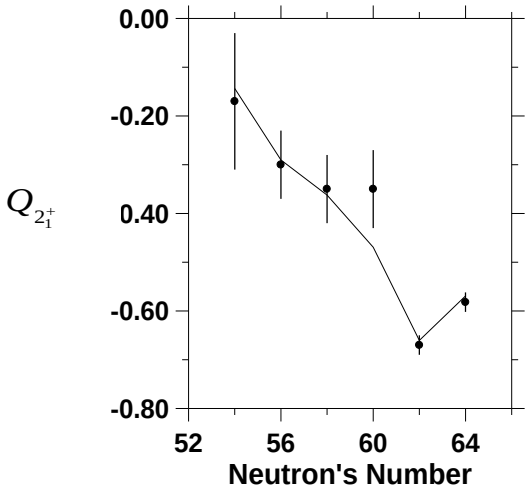

Fig. 4: The calculated quadrupole moments (the solid line) for the first excited 2_1^+ state compared with those of experimental data (solid circles) [23, 28, 29] in the $Ru-$isotopes.

Conclusions:

The analysis performed in this study makes it possible to draw the following:

1. The low-lying experimental energy levels of the ground state bands in all $Ru-$isotopes are very well reproduced by those of calculated results of IBM-2 as seen in Fig. (1).
2. In general, the calculated results of IBM-2 for the $B(E2)$ transitions in all considered $Ru-$isotopes show an increase in their values with the increasing of the neutron numbers since this behavior agree quite well with those of the experimental data. In addition, the calculated $B(E2;2_2^+ \rightarrow 0_1^+)$ of IBM-2 is not in agreement with the experimental results throughout all considered $Ru-$isotopes. This discrepancy may be attributed to the considering a fixed value of effective charge.
3. The experimental quadrupole moments of the first excited 2_1^+ state $Q_{2_1^+}$ are very good described by the calculations of IBM-2 throughout all considered $Ru-$isotopes. Both the calculated and the experimental $Q_{2_1^+}$ show a general feature of increasing their values in the negative quadrupole moment with increasing the neutron number.
4. We could not draw an explicit conclusion for the $B(M1)$ transitions in the considered $Ru-$isotopes because of the lack of the experimental data in these isotopes. However, It is concluded that the properties of $M1$ operator are exclusively determined by the parameters of g_π and g_ν factors since using the choice of g_π=0.25 μ_N and g_ν=0.085 μ_N in the calculations of IBM-2 produces results for the magnetic dipole moments $\mu_{2_1^+}$ [denoted by Th1 in Table (2)] do not agree with the experiment throughout all considered $Ru-$isotopes while the choice of g_π=1.00 μ_N and g_ν=0.42 μ_N gives results for $\mu_{2_1^+}$ [denoted by Th2 in Table (2)] agree quite well with the experiment throughout all considered $Ru-$isotopes.

References

1. Hicks S.F., Vanhoy J.R.,and Yates S.W., 2008.Fragmentation of mixed-symmetry excitations in stable even-even tellurium nuclei, Phys.Rev., C78, 54320
2. Falih H., 2009. Mixed symmetry states and decays of odd-A Xe to I isotopes, Phys.Rev., C80, 14306.
3. Genilloud L., Brown T., Warr N., Tolie J. and Yates S., 2001. Characterization of the 3-phonon region Ru-100, Nucl.Phys., A683, 287.
4. Gade A.,Wiedmnover I., Meise H., Gelberg A. and Vonbrentano P., 2002.Decay properties of low-lying collectives states in Ba-132, Nucl.Phys., A697, 75.
5. Pasternak A., Sasaki Y., Efimov A., Mikhajlov V., Shinohara N. and Liu Z., 2001.DSA lifetime measurements and structure of positive parity bands of X-120,

European Physical Joarnal, A9, 293.
6. Saha A., Seth K., Casey L., Godman D., Stuart J. and Scholten O., 2001, Phys.Rev., C6302, 4309.
7. Fransen C., Pietralla N., Dewald A., Gableske J., Lisetskiy A. and Werner V., 2001, Phys.Letts., B 506, 219.
8. Saha A., Seth K., Casey L., Seth R., Stuart J. and Scholten O., 2001, Phys.Letts., B 132, 51.
9. Carr J., Petrovich F., Philpott R., Scholten O. and Mcmanus H., 1985, Phys.Rev.Letts., 54, 11985.
10. Fransen C. et. al., 2001.Identification of mixed-symmetry states in Mo-44, Acta Physica Polonica, B 32, 777.
11. Arima A. and Iachello F., 1981.Collective nuclear states as symmetric couplings of proton and neutron excitations, Ann.Rev.Nucl.Part.Sci., 31, 75.
12. Sambataro M., Scholten O., Dieperink A. and Piccitto G., 1984.On magnetic dipole properties in the neutron-proton model, Nucl.Phys., A423, 333.
13. Otsuka T., Arima A. and Iachello F., 1978.New symmetry in the sd model of nuclei the group o(6), Nucl.Phys., A 309, 1.
14. Gelder P., Jacob E. and Frenne D., 1983, Nuclear Data Sheets, 39, 533.
15. Gelder P., Erenne D. and Jacobs E., 1974, Nucl Data Sheets, 11, 302.
16. Samuelson L.E., Auble R.L. and Mcharris W.C., 1976, Nuclear Data Sheets, 19, 19.
17. Lipas P., Hammaren E. and Frenne D., 1982, Nuclear Data Sheets, 35, 451.
18. Van Isacker P., Jacob E. and Frenne D., 1984, Nuclear Data Sheets, 41, 332.
19. Rachavan P., 1980, Nuclear Data Sheets, 30, 346.
20. Frenne D., Gelder P. and Jacob E., 1988, Nuclear Data Sheets, 53, 78.
21. Haese R.L., Bertrand F.H., 1982, Nuclear Data Sheets, 37, 292
22. Raman et al., 1989, Atomic Data And Nuclear Data Tables, 42, 1, 15.
23. Bockisch A., Gelberg A., and Kaup U., 1979.Reorientation effect measurement and multiple coulomb excitation in ^{102}Ru , Z.Physika., 292, 265.
24. Frenne D., et al., 1978. β^- decay of ^{102}Te , Physical Review C, 18, 1, 486.
25. Summrer K., et al., 1978.Angular correlations of $\gamma-$ray transitions in ^{104}Ru , Nuclear Physics, A308, 1.
26. Summrer K., et al., 1980.Levels in $^{106}Ru\ and\ ^{108}Ru$, Nuclear Physics, A339, 74.
27. Van P.,and Heyde K., 1982.Interpretation of the A=100 transitional region in the frame work of the IBM model, Physical Review C, 25, 1, 650.
28. Landsberger S., et al., 1980.Quadrupole moments of the first excited states of $^{96}Ru,^{98}Ru,^{100}Ru,^{102}Ru,and^{104}Ru$, Physical Review C, 121 2, 588.
29. Hirata H., Salem S.,and Dietzsch O., 1998.Electromagnetic properties of the first 2_1^+ excited states in $^{100,102,104}Ru$, Phys.Rev., C57, 76.

30. Stngh B., and Taylor W., 1970.Directional correlation and multipole mixing of the gamma transitions in ^{102}Ru, Nuclear Physics, A155, 70.
31. Krone K.S., 1984.Coulomb excitation of states in the even-mass ruthenlum nuclei with $^{16}O\ and\ ^{4}He$ ion, Physical Review C, 10, 3,1197.
32. Stachei J., Broden K., and Eriksen D., 1984.The collective structure of $^{106,108}Ru$, Z.Phys. Atomic and Nuclei, 316, 105

دراسة الخواص النووية لنظائر Ru استخدام IBM

الطاف عبد المجيد الرحماني*

*قسم الفيزياء , كلية العليوم للبنات , جامعة بغداد

الخلاصه:

لقد تم استخذام انموذج البوزونات المتفاعله (IBM-2) لعمل دراسة تخطيطية لنظائر الروثنيوم (Ru) المتواجدة ضمن منطقة العدد الكتلي $A=100$ و العدد النيوتروني $54 \le N \le 64$. لقد تم ايجاد اعلومات المؤثر الهاملتوني والتي اعطت نتائج مقبولة لطاقات التهيج مقارنة مع النتائج العملية. لقد تم استخذام قيم ثابتة لكل من الشحنات المؤثرة ($e_\pi = e_\nu = 0.102\ e.b.$) وكذلك للقيمة المؤثرة للأعلومتين ($g_\pi = 1.0\ \mu_N$ و $g_\nu = 0.42\ \mu_N$) لجميع نظائر Ru قيد الدراسة. ان النتائج المحسوبة لكل من العزم الكهربائي لرباعي القطب والعزم المغناطيسي لثنائي القطب للحالة (2_1^+) و الأنتقالات الكهربائية الرباعية $B(E2)$ و الأنتقالات المغناطيسية ثنائية القطب $B(M1)$ ونسبة الخلط $\delta(E2/M1)$ تتفق بصورة مقبولة مع النتائج العملية.